Chitin binding study of a lytic polysaccharide monooxygenase from the marine bacterium *Vibrio campbellii*

Yong Zhou [1] and Wipa Suginta [1,*]

[1] School of Biomolecular Science and Engineering (BSE), Vidyasirimedhi Institute of Science and Technology (VISTEC), Payupnai, Wangchan Valley, Rayong 21210, Thailand; yong.z_s18@vistec.ac.th

* Correspondence: wipa.s@vistec.ac.th;

Abstract: The enzymatic degradation of naturally abundant polysaccharides has received much attention by biotechnological industries, most notably for first (starch) and second (cellulose/chitin) generations of biofuel production. Lytic polysaccharide monooxygenases (LPMOs) are copper-dependent enzymes that are capable of oxidative cleavage of recalcitrant polysaccharides, such as chitin or cellulose and they may also play a critical role in bacterial infections. Despite the importance of LPMOs in biomass conversion and a large number of LPMO genes that have been identified from various microorganisms, only a few LPMOs have been well studied so far. Therefore, further characterization of these proteins is thus of interest. In the present study, a chitin-active LPMO family AA10 from the marine bacterium, *Vibrio campbellii* ATCC BAA-1116 (formerly *Vibrio. harveyi*), named *Vh*LPMO10A, is described. This enzyme consists of 487 amino acids, comprising a signal peptide followed by an *N*-terminal family AA10 LPMO catalytic domain, an uncharacterized α+β domain and a *C*-terminal CBM carbohydrate-binding domain. This enzyme was successfully produced and expressed at a high level in the exogenous *E. coli* strain BL21(DE3) host cells. *Vh*LPMO10A was shown to bind different chitin polymeric substrates with different extents of binding capacity. The results obtained may provide a further understanding of this new member of chitin-active LPMOs.

Keywords: Chitin; Lytic polysaccharide monooxygenase; *Vibrio campbellii;* Chitin-binding assay.

1. Introduction

Chitin is an insoluble homopolysaccharide composed of *N*-acetylglucosamine, GlcNAc, units linked together β-1,4-glycosidic linkages. It is one of the most important and highly recalcitrant biopolymers widely occurring in nature. It is abundantly distributed in nature as the main component of the exoskeleton of invertebrates, such as crustaceans and insects(1–3). It is also found in the cell walls of fungi, yeast, and green algae (4, 5). The main use of chitin is as a raw material to produce chitin-derived products, such as chitosan oligosaccharides, and glucosamine (1, 6–8).

In nature, efficient recycling of chitins was carried out by microorganisms that generally utilize the chitinolytic enzyme system including non-processive endochitinases in tandem with processive exo-type (9–11). Using enzymes and/or microorganisms to degrade chitin polysaccharides offers a more environmentally friendly measure to eliminate this waste (12). Previous studies pointed out that some bacteria produce polysaccharide binding proteins that are capable of increasing substrate accessibility and activity of hydrolytic enzymes (13). Recent studies highlighted that some of these carbohydrate-binding proteins, such as LPMOs, possess enzyme activity, which could catalyze the cleavage of glycosidic bonds of polysaccharides via an oxidative mechanism, generating a series of oxidized oligosaccharides (14, 15). LPMOs are classified in the Carbohydrate Active Enzymes (CAZy) database (www.cazy.org) among the Auxiliary Activity (AAs), where they

are currently grouped into seven families AA9, AA10, AA11, AA13, AA14, AA 15 and AA16 (16–18). Functionally, AA10 LPMOs can be divided into two subclasses: chitin-oxidative (i.e., *Sm*CBP21 from *Serratia marcescens*) and cellulose-oxidative LPMOs (i.e., $CelS_2$ from *Streptomyces coelicolor* A3) (13, 16, 19–21). AA10 LPMOs are copper-dependent enzymes, comprising a solvent-exposed mononuclear type-2 copper binding active site, which is a T-shaped coordination sphere named the histidine-brace, where two histidine residues provide three nitrogen ligands; two are from the *N*-terminus histidine side chains and one from the terminal amine (9, 20, 22, 23).

Hydrolytic enzymes that attack chitin frequently contain at least one non-catalytic carbohydrate-binding module or CBM (9, 24). The CBM was first identified in cellulases, and its function was to recruit the cognate enzymes into proximity with their target substrates, thus elevating the level of catalysis (25). It has also been proposed that some chitin-specific CBM can direct the chitinolytic enzymes to the regions of the animal exoskeleton that are particularly accessible to biological attack, whereas it has also been shown that these modules can also modulate enzyme specificity (26–28). CBM truncation studies have been reported for both LPMO9s and LPMO10s (25). Comparison of the performance of LPMOs with and without CBMs have shown that the deletion of CBMs reduced LPMO's binding capacity to crystalline substrates, especially at low substrate concentrations (29). Therefore, CBMs may affect substrate specificity by promoting the binding of LPMOs to the appropriate substrates.

Vibrio spp. are Gram-negative bacteria that have a curved-rod shape and polar flagella with sheaths. Some of these bacteria, such as *Vibrio campbellii* (formerly *Vibrio. harveyi*) ATCC BAA-1116 and *Vibrio fischeri*, are bioluminescent through a cellular mechanism that is regulated by quorum sensing (30, 31). *Vibrio spp.* are facultative anaerobes that are widespread in coastal waters and ocean sediments and pathogens of aquatic fish and invertebrates, including crustacean and zooplankton (32–34). The previous studies by *Suginta* and colleagues (35, 36) reported a major endochitinase, namely *Vh*ChiA, and an exolytic *β-N*-Acetyl-glucosaminidase or *Vh*GlcNAcase from *Vibrio campbellii*. The N-terminal CBM domain in *Vh*ChiA was able to bind with various types of insoluble chitins (37). The binding affinity of the CBM was significantly decreased compared to that of the intact chitinase molecule. The result suggests that the two functional domains (the catalytic domain and the CBM domain) of *Vh*ChiA work synergistically to guide the polymeric substrate into the substrate-binding cleft (37).

In this study, we carried out recombinant expression and purification of *Vh*LPMO10A in the *E. coli* expression host. The binding properties of the intact *Vh*LPMO10A and the CBM domain of *Vh*LPMO10A towards different chitin substrates were characterized. The results obtained from this study may help to shed light on the functional role of the CBM domain of *Vh*LPMO10A in accessing chitin substrates from different marine organisms.

2. Materials and Methods

Materials and Chemicals. Solid α-chitin from crab and shrimp and β-chitin from squid pen, respectively, were purchased from Marine BioResources Co. Ltd. (Samut Sakhon, Thailand). High molecular weight (HMW) chitosan type A, type B and mixed chitosan oligosaccharides were purchased from Koyo Chemical Co., Ltd. (Osaka, Japan). Mixed chitin oligosaccharides were purchased from Seikagaku Biobusiness Co., Ltd. (Tokyo, Japan). The gene encoding *Vh*LPMO10A was synthesized (GeneScript, Piscataway, NJ) after codon optimization for *E. coli*. expression system and inserted into the vector pET22b(+) in frame with the C-terminal $(His)_6$-tag. HiTrap Q HP column (∅ = 1 cm x 5 cm) and 16/60 Superdex™ s-200 (∅ = 16 cm x 60 cm) were purchased from GE Healthcare (Chicago, IL). All other reagents were of analytic grade unless stated otherwise.

Expression and purification of recombinant *Vh*LPMO10A. The expression plasmid, pET22b(+)/*lpmo,* was transformed into the *E. coli* BL21(DE3) Star cells (Invitrogen) by heat-shock and spread on the LB (Luria-Bertani) agar plate containing 100 μg/ml ampicillin for

positive selection. Single positive colony was picked and transferred into 50 ml LB media containing the same concentration of ampicillin overnight at 37 °C, 180 rpm. Afterward, 1% of the overnight culture was inoculated in 6 flasks of 650 mL LB medium (total of 4 L), containing the supplement, IPTG, for induction. Briefly, cells were cultured at 37 °C in an orbital shaker (200 rpm) for 3-4 h until OD_{600} of ~0.6 to 0.7, followed by induction with 0.4 mM isopropyl β-d-1-thiogalactopyrano-side (IPTG) at 20 °C for 16 h with shaking 180 rpm. The cell was pelleted by centrifugation (20 mins at 8,000 rpm) at 4°C and resuspended in lysis/binding buffer (10 mM imidazole and 300 mM NaCl, in 20 mM Tris–HCl pH 6.5) containing 100 μM phenylmethylsulfonyl fluoride (PMSF), 1.5% glycerol and 1mg/ml lysozyme. The cell suspension was disrupted using a Vibra cell Ultrasonic Processor (Sonics, Newton, Ct, USA), by applying repeated cycles of 10s on 20s off for 30 mins using 20% amplitude. The cells were kept on ice at all times. Cell debris was removed by centrifugation at 18,000 rpm for one hour at 4°C. The resulting supernatant was immediately applied to a Nickel-based TALON® metal affinity resin (Clontech Laboratories, Inc., A Takara Bio Company, Mountain View, CA, USA) run under gravity at 4°C following the manufacturer's instructions (https://www.takarabio.com/). The column was pre-equilibrated with 5 column volumes (CVs) of the equilibration buffer (20 mM Tris-HCl, pH 6.5 containing 300 mM NaCl and 10.0 mM Imidazole). After sample loading, the column was washed by 40 CVs of the equilibration buffer containing 10 mM imidazole and the bound proteins were eluted by the same buffer but containing 150 mM imidazole. The purity of the target protein was analyzed by 12% SDS-PAGE, based on the method reported by *Laemmli et al* (38). The eluted protein fractions were pooled and dialyzed against imidazole and NaCl by 20 mM Tris-HCl buffer, pH 6.5 and the resulting protein was filtered with a 0.45-μm membrane filter (Pall® Corporation, New York, USA). Using an AKTA Purifier (GE Healthcare) protein purification system, the filtrate was applied on a 5-mL HiTrap Q HP column equilibrated with the dialysis buffer. After washing the column with 10 CVs of the same buffer, the adsorbed proteins were eluted with linear gradient elution from 0 to 1 M NaCl in the same buffer. The protein fractions were pooled and finally purified by a gel-filtration column of 16/60 Superdex™ S-200. After confirming a single protein band by SDS-PAGE, the purified *Vh*LPMO10A fractions were stored at 4 °C and used for subsequent experiments. Protein concentration was determined by reading absorbance at 280 nm, using the theoretical extinction coefficient calculated using *ExPASy* server online, 86,665 $M^{-1}{\cdot}cm^{-1}$.

Copper saturation of *Vh*LPMO10A. Before enzyme activity assays, *Vh*LPMO10A was saturated with $CuSO_4$ solution in accordance with the protocol from the previous study by *Loose et al*(39). Briefly, the enzyme was incubated for 2 hours at 0°C with $Cu(II)SO_4$ at a molar ratio of 1:2 (enzyme : copper). After saturation, the enzyme was applied again to a gel-filtration column of 16/60 Superdex™ S-200 using 20 mM Tris-HCl buffer, pH 6.5 as running buffer to remove excess $Cu(II)SO_4$. X-ray absorption spectroscopy (XAS) technique at *Beamline 1.1W* in Synchrotron Light Research Institute (Public Organization, Thailand), was applied to scan the copper-binding situation of *Vh*LPMO10A with 100 mM $Cu\ (II)SO_4$ as control.

Preparation of chitin substrates. The colloidal chitins were prepared by the method of *Gustav Vaaje-Kolstad et al* (39) with a small modification. Briefly, 10 g of chitin shell particles was stirred overnight with 100 mL of 33% HCl and the pH was adjusted to ~7.0 by the addition of NaOH. The acid-treated chitin suspension was centrifuged at 8,000 rpm, 4°C for 20 mins, and the chitin pellet was collected and resuspended in Milli-Q water (Millipore). The washing step was repeated five times and the pure colloidal chitin pellet was dried until powder under 50°C oven and then stored at 4°C until further use.

Chitin-binding assay. The binding assay was adapted from a previously related reported protocol with small modifications explained hereinafter (37). The ability of *Vh*LPMO10A to bind to various types of chitin (colloidal α and β-chitins, chitosan type A, type B and chitosan oligosaccharides) was tested and compared with that of the WT *Vh*ChiA from previously reported by *Suginta et al.*(36, 37). The reaction mixture (200 μL)

contains 5 mg/mL chitin and 10 μg *Vh*LPMO10A in 20 mM Tris-HCl buffer, pH 6.5 or *Vh*ChiA in 100mM sodium acetate, pH 5.0. The reaction mixtures were incubated at 0°C with constant agitation at 300 rpm for various times (0, 2.5, 5, 10, 15, 30, 45, or 60 mins), and then the chitin-bound protein was collected by centrifugation at 16,000 *g* at 4°C for 10 mins. The concentration of the unbound protein remaining in the supernatant was determined by Bradford's method.

Chitin-binding by SDS-PAGE analysis. According to the previous report by *Dafni et al.*(39), binding of *Vh*LPMO10A was assayed in 100-μL reactions containing 10 mg/mL of substrate (α-chitin from crab and shrimp, β-chitin from squid pen) and 0.2 mg/mL purified *Vh*LPMO10A in 20 mM Tris-HCl buffer, pH 6.5 or *Vh*ChiA in 100mM sodium acetate, pH 5.0, respectively. Control reactions were identical but contained no substrate. The reactions were incubated at 0°C with constant agitation at 300 rpm for 60 mins. Subsequently, the substrate was sedimented by centrifugation at 16,000 *g*, 4°C for 10 mins. The supernatant (containing the non-bound protein) was decanted off and kept on ice until analysis. The pellet was washed twice with 500 μL of buffer, followed by resuspension in 50 μL of SDS-PAGE sample buffer (Invitrogen) and 10 min of incubation at 75°C. In total, 5 μL of supernatant and 10 μL of the proteins that had remained bound to the pellets were analyzed using SDS/PAGE Mini-Protean Stain-free 10% gels.

Effect of pH on chitin-*Vh*LPMO10A interactions. The 200-μl reaction mixture contained 5 mg/mL colloidal β-chitin from squid pen and 10 μg *Vh*LPMO10A or *Vh*ChiA in citric acid/sodium phosphate buffer, with pH adjusted to cover the range 3–8 for *Vh*ChiA and 20 mM Tris-HCl buffer, with pH adjusted to cover the range 8–10 for *Vh*LPMO10A. The reaction mixture was incubated at 0°C with constant agitation at 300 rpm for 60 mins, and then the unbound protein remaining in the supernatant was determined as described in the previous section.

All experiments were carried out in triplicate and all the data were analyzed in *PrismGraphPad v. 9.0*.

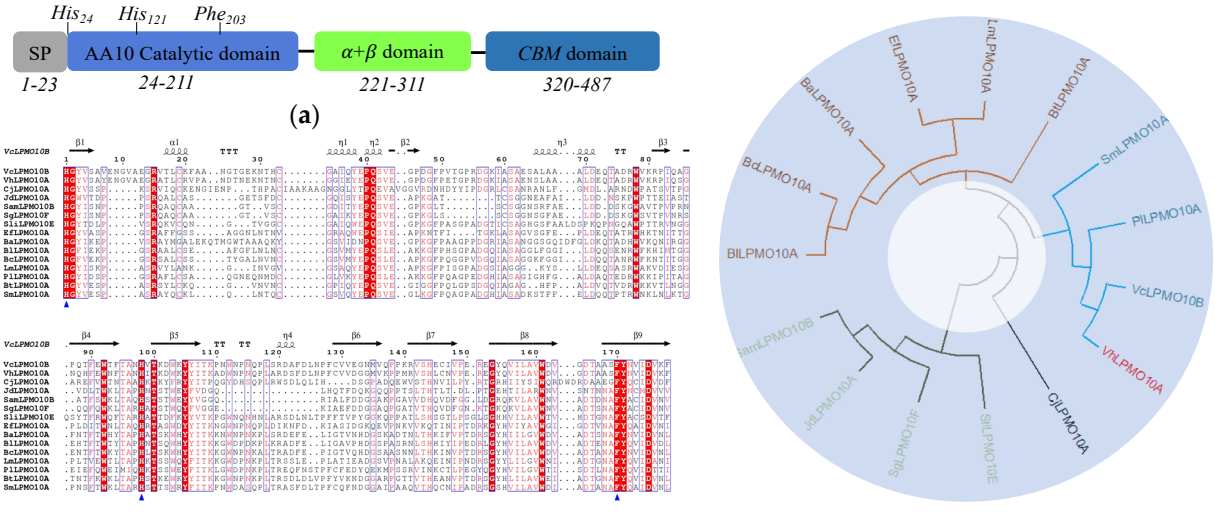

Figure 1. Sequence analysis of *Vh*LPMO10A. (**a**), domain architecture of *Vh*LPMO10A. The full-length enzyme contains a signal peptide that is cleaved off during secretion resulting in the mature enzyme that possesses an N-terminal AA10-type catalytic domain (Cat), followed by an uncharacterized α+β domain and a C-terminal carbohydrate-binding domain (CBM) colored in blue, green and skyblue, respectively. The three domains are separated by two poly-serine linkers (PSL). The modules and linkers are scaled according to the number of amino acids they contain. (**b**), multiple sequence alignments of 15 bacterial Chitin-active LPMOs. (**c**), Phylogenetic tree of *Vh*LPMO10A with other bacterial chitin-active LPMOs.

3. Results

3.1. Sequence Analysis of VhLPMO10A

Using known chitin-active LPMOs from 14 bacterial species as multiple alignment templates, *Vh*LPMO10A from *V. campbellii* was successfully identified by bioinformatics, and then was used to generate the phylogenetic tree (Figure 1). *Vh*LPMO10A consists of 487 amino acids comprising a signal peptide (residues 1–23) that is cleaved off during secretion, followed by an N-terminal family AA10 LPMO catalytic domain (residues 24–201), an uncharacterized α+β domain (residues 221–311), and a C-terminal CBM carbohydrate-binding domain (residues 320–487) (see Fig. **1a**). Multiple sequence alignments of the selected bacterial chitin-active AA10 LPMO sequences (catalytic domains only) show that *Vh*LPMO10A contains three residues consisting of two histidine and one phenylalanine residues involving in catalysis. Compared to cellulose-active AA10 LPMO, it comprises tyrosine as the third catalytic residue (Fig. **1b**). Phylogenetic analysis of the selected AA10 chitin-active LPMO sequences (catalytic domains only) shows that *Vh*LPMO10A is in the same cluster with the established clade II in which is known to degrade α-/β-chitin at C1-bond (Fig. **1c**). The most similar characterized chitin oxidizing *Vc*LPMO10B shows 69.91% sequence identity to the *Vh*LPMO10A full-length sequence. The sequence analysis in combination with the chitin-binding data (see below) demonstrated that *Vh*LPMO10A is a chitin-specific LPMO.

3.2. Copper-dependent active sites of chitin-active LPMO10s

The three-dimensional structure of *Vh*LPMO10A was predicted by the SWISS-MODEL online (https://swissmodel.expasy.org/interactive) and then aligned with the active site with the known 3D structure *Vc*LPMO10B (PDB id: 2xwx). The active site of *Vh*LPMO10A is similar to *Vc*LPMO10B, both containing a copper ion coordinated by two histidine residues in a T-shaped histidine brace (Fig. **2**). In addition to two histidine residues, there is the third key residue, phenylalanine, which is known as a specific catalytic residue on chitin, not on cellulose, in bacterial AA10 LPMOs.

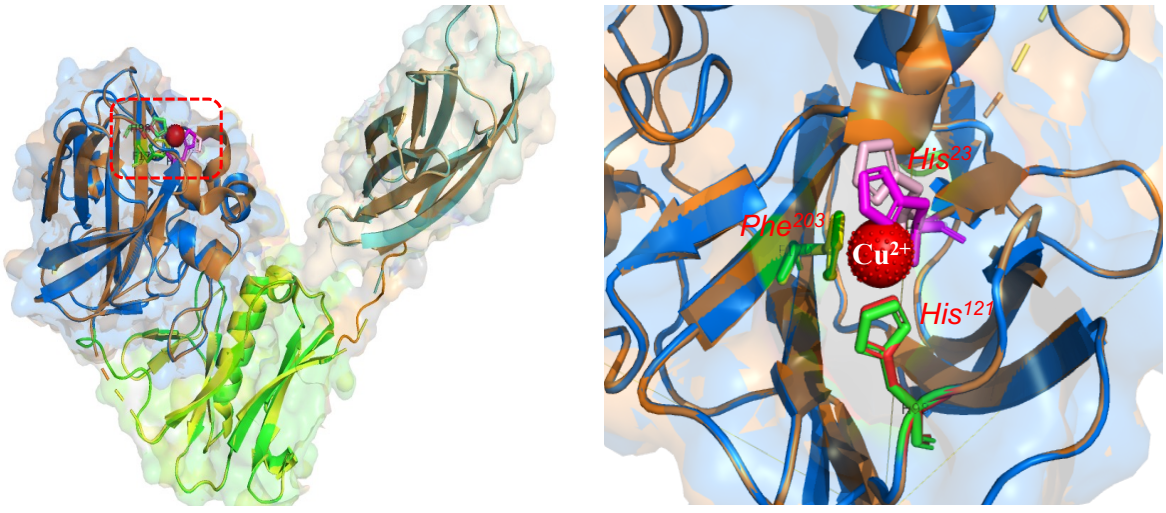

(**a**) (**b**)

Figure 2. Copper-dependent active sites of chitin-active LPMO10s. (**a**), superposition of the *Vh*LPMO10A copper active site with chitin-active *Vc*LPMO10B (PDB id: 2xwx). Carbon atoms in the two enzymes are colored blue in the catalytic domain, green in α+β domain and orange in the CBM domain for *Vh*LPMO10A but orange, yellow and cyan for *Vc*LPMO10B, respectively. (**b**), the copper active site of *Vh*LPMO10A compared to *Vc*LPMO10B. The catalytic residues were colored in pink (His^{23}) and red (His^{121}) and yellow (Tyr^{203}) for *Vh*LPMO10A.

3.3. Expression, purification and copper saturation of VhLPMO10A

The recombinant chitin-active *Vh*LPMO10A has been successfully expressed at a high level in *E. coli.* BL21(DE3) expression strain and the recombinant protein were purified to homogeneity by three-step chromatography. Figure **3a** shows the SDS-PAGE profile of *Vh*LPMO10A after being purified by Ni^{2+}-affinity chromatography. The molecular weight of the target protein was slightly above 55 kDa, consistent with the molecular mass of *Vh*LPMO10A predicted from its 464-amino acid sequence (51,141.22 Da). Figure **3b** is the gel filtration profile run on a 16/60 Superdex™ S-200 column. The eluted fractions (17-20) were analyzed by SDS-PAGE and Coomassie staining (Fig.3b, inset) showed a single band of the protein after gel filtration.

To verify the copper-binding property of *Vh*LPMO10A, 0.7 mM protein was incubated with 1.4 mM Cu(II)SO_4 at 0°C for 2 hours. After saturation, the enzymes were applied again to a gel-filtration column of 16/60 Superdex™ S-200 using 20 mM Tris-HCl buffer, pH 6.5 as running buffer to remove excess Cu(II)SO_4. XAS technique was applied to scan the copper-binding state of *Vh*LPMO10A using 100 mM CuSO4 as control (the data of *Vh*LPMMO10A without Cu(II) not shown). The result indicated the assigned peak corresponding to Cu(II) in the LPMO sample containing $CuSO_4$ at the energy range between 8975 and 9000 eV, which was corresponded to the control signature (CuSO4), indicating that free Cu(II) spontaneously bound to the LPMO enzyme (Fig.**3c**).

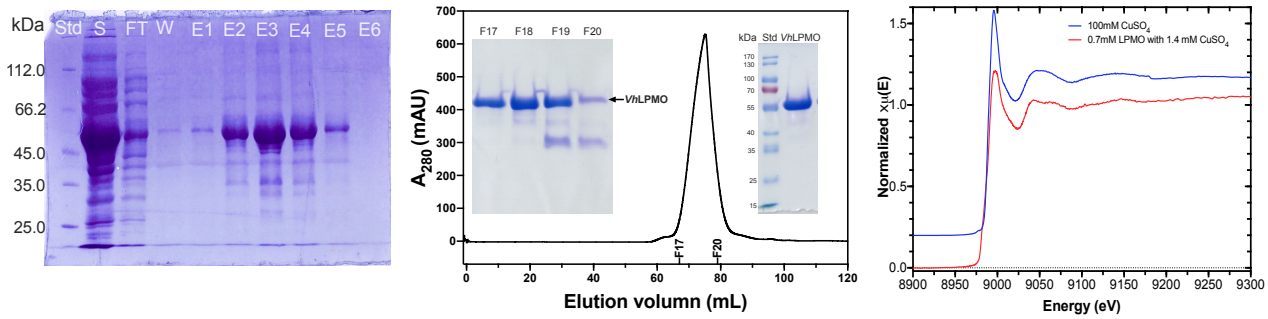

(**a**) (**b**) (**c**)

Figure 3. Purification and copper binding study of *Vh*LPMO10A. (**a**), purification of recombinant *Vh*LPMO10A by Ni^{+}-affinity chromatography. Std, protein standard marker; S, crude protein from supernatant; FT, Flow-through; W, Wash; E1-6, elute protein. (**b**), gel filtration profile of *Vh*LPMO10A with an SDS-PAGE gel, stained with Coomassie Brilliant Blue R-250, of the eluted peak from F17 to F20 (insert left) and after concentration (insert right). (**c**), X-ray absorption spectroscopy of copper in *Vh*LPMO10A colored in red and 100mM Cu(II)SO_4 as standard control.

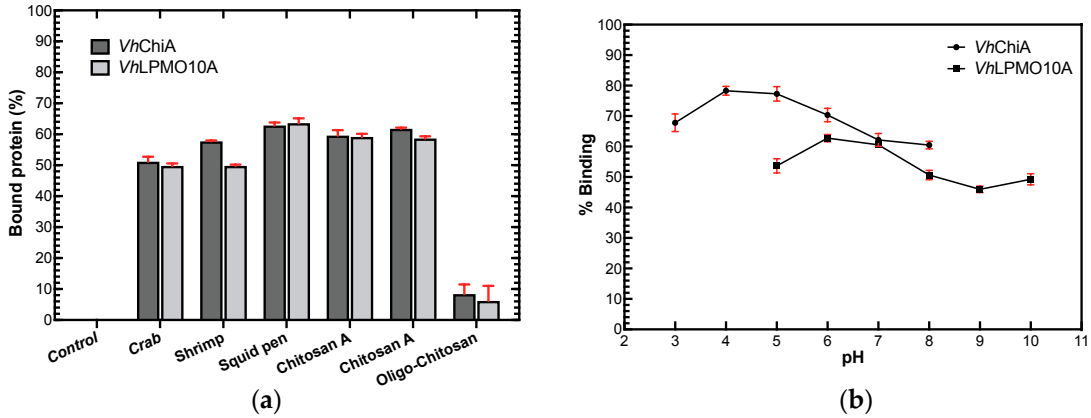

(**a**) (**b**)

Figure 4. Chitin-binding assays. (**a**), binding of *Vh*LPMO10A (dark grey bar) and *Vh*ChiA (light grey bar) to insoluble chitin/chitosan and soluble oligo-chitosan. After binding at 0 °C and pH 6.5 for *Vh*LPMO10A and pH 5.0 for *Vh*ChiA for 60 min. (**b**), effects of pH on the binding of *Vh*LPMO10A (filled circles) and *Vh*ChiA (filled squares) to colloidal β-chitin. After incubation of the protein with chitin in a buffered solution at different pH values for 60 min. Chitin was removed by centrifugation and the concentration of the unbound protein in the supernatant was determined by Bradford's method.

3.4. Chitin-VhLPMO10A binding study

Next, we directly measured chitin-binding to determine the substrate specificity of *Vh*LPMO10A. Measurement on the binding of various types of insoluble chitins and their derivatives (chitosan and oligo-chitosan) and compare the results of *Vh*LPMO10A (dark gray) and *Vh*ChiA (light gray) (Fig.**4a**). Both proteins can bind all forms of insoluble polysaccharides but can slightly bind a few soluble oligo-chitosan, with the percentage of binding is about 10-fold lower than that of insoluble chitin and its derivatives. Figure **4b** shows the pH-dependence of the binding of *Vh*LPMO10A and *Vh*ChiA to colloidal β-chitin from the squid pen. Both forms of protein can interact with chitin polymers in a wide pH range, but at pH 4-5, the binding fraction is the largest on *Vh*ChiA (this enzyme is known to bind chitin polymer with high efficiency) and at pH 6-7 on *Vh*LPMO10A. Similarly, in the entire pH range, the binding fraction of *Vh*ChiA is slightly greater than that of *Vh*LPMO10A.

3.5. Determination of chitin binding specificity

Upon incubation with various chitin from different sources, the binding preference of *Vh*LPMO10A proved to be relatively broad as strong binding was observed to different chitin polymers compared to *Vh*ChiA. We also carried out time-course binding experiments to determine the binding specificity of *Vh*LPMO10A on α-/β-chitin. The results show a plot of free (unbound) protein remaining in the supernatant over a period of 60 min. The binding of *Vh*ChLPMO10A to both types of chitins occurred rapidly for the first 10 mins after mixing and reached equilibrium with 60 min of incubation, but only weak binding to crystalline chitosan was observed. In addition, the binding assay of *Vh*LPMO10A on β-chitin from squid pen is greater and faster with 33% than α-chitin from shrimp (Fig.**5**).

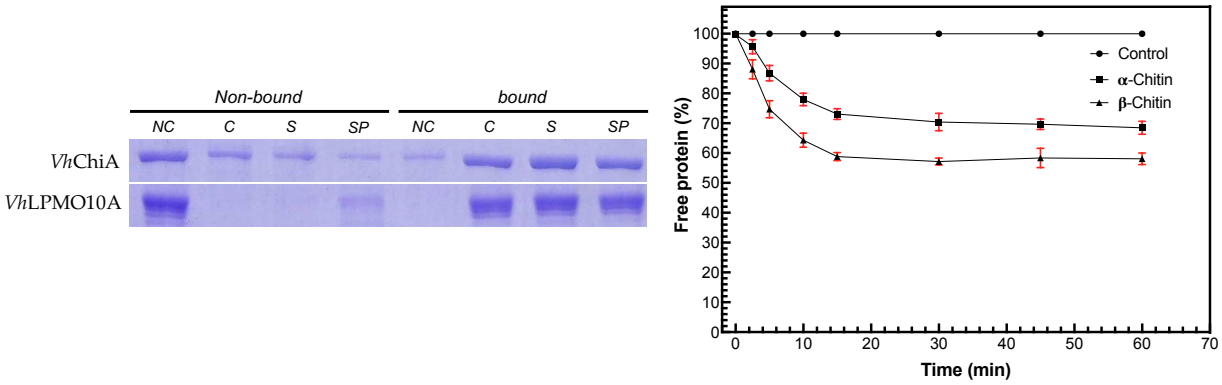

(**a**) (**b**)

Figure 5. Binding specificity of *Vh*LPMO10A on chitin. (**a**), The amount of *Vh*LPMO10A or *Vh*ChiA (0.2 mg/mL) bound to 10 mg/mL α-/β-chitin is depicted in comparison to the non-bound protein remaining in the supernatant after 60 mins of incubation with the substrates. *NC*, control sample with no substrate. The faint band observed in the (*NC*) indicates that *Vh*LPMO10A or *Vh*ChiA binds to the inner walls of the test tube (protein precipitation was not observed). *C*, crab; *S*, shrimp; *SP*, squid pen. Results were reproduced in at least three independent sets of experiments. (**b**), time-courses of binding of *Vh*LPMO10A to chitin substrate (α-chitin from shrimp). The binding reaction was carried out at pH 6.5 and 0 °C for 0–60 min with constant shaking. The concentration of the bound enzyme (E_b) was calculated from the difference between the initial protein concentration (E_t) and the unbound (free) protein concentration (E_f) after binding.

4. Discussion

The CBM domain of LPMOs has been proposed to be crucial for their interaction with recalcitrant polysaccharides such as chitin biopolymers. In our previous study, we reported that the CBM domain of *Vh*ChiA was essential for the initial interaction of a chitin strand with chitinase. the related structural evidence suggested that the chitin-binding domain of GH-18 chitinases facilitated a sliding process that guided the bound chitin

chain toward the catalytic domain, and then its entry into the substrate-binding groove. On the other hand, short chitooligosaccharides did not require interaction with the chitin-binding domain to reach the active site.

In the present study, we set out to identify, express and examine the chitin-binding properties of the isolated AA10 LPMO from the marine *Vibrio* bacteria. A full-length gene encoding residues 23–487 of *Vh*LPMO10A was produced and expressed at a high level in exogenous host cells, *E. coli* strain BL21(DE3). The protein domain was purified to homogeneity by Ni^{2+}-NTA affinity chromatography followed by gel filtration chromatography, yielding about 16 mg of purified protein per liter of bacterial culture.

To determine the binding properties of *Vh*LPMO10A compared to the known characterized *Vh*ChiA that contains the chitin-binding domain, we performed direct chitin-binding assays, the results of which consistently showed that *Vh*LPMO10A interacted with insoluble chitin with slightly greater than with insoluble chitosan. In addition, *Vh*LPMO10A showed the preferred substrate was colloidal β-chitin over α-chitin, presumably because of its higher purity and a lower percentage of recalcitrance compared to α-chitin, thus allowing access to individual sugar chains by the protein domain.

5. Conclusions

In conclusion, the present study reports the chitin-binding study of an AA10 LPMO from the marine bacterium *Vibrio campbellii*, which provides new insights into the substrate-binding properties of a new member of LPMOs on chitin degradation in the *Vibrio* system. Further substrate degradation and structural investigation will help to elucidate the catalytic mechanism of recalcitrant polysaccharide oxidation on a molecular level.

Supplementary Materials: All materials are contained within this article.

Author Contributions: Y. Z. conducted all the experiments, generated and analyzed the data, wrote the first article draft, and prepared all the figures. W. S. guided and revised the manuscript and managed the whole project completion. All authors have read and agreed to the published version of the manuscript.

Funding: This research was full funded by Vidyasirimedhi Institute of Science and Technology (VISTEC), Thailand by the full-time PhD scholarship to Y.Z. WS was supported by Vidyasirimedhi Institute of Science and Technology and Thailand Research Fund through The Basic Research Grant (BRG610008) and Thailand Science Research and Innovation through Global Partnership Grant (Contract no: PMUB-P5-63-B20PIC_WIS_CHU-PMB010).

Institutional Review Board Statement: Not applicable.

Informed Consent Statement: Informed consent was obtained from all subjects involved in the study

Data Availability Statement: All data are contained within this article.

Acknowledgments: This work was full financially supported by Vidyasirimedhi Institute of Science and Technology (VISTEC), Thailand. We thank the assistance of Dr. *Suttipong Wannapaiboon* on XAS at Synchrotron Light Research Institute (Public Organization), Thailand.

Conflicts of Interest: The authors declare no conflict of interest.

References

1. Gooday, G. W. (1990) Physiology of microbial degradation of chitin and chitosan. Biodegradation. 1, 177–190
2. Forsberg, Z., Bissaro, B., Gullesen, J., Dalhus, B., Vaaje-Kolstad, G., and Eijsink, V. G. H. (2018) Structural determinants of bacterial lytic polysaccharide monooxygenase functionality. J. Biol. Chem. 293, 1397–1412
3. Wang, D., Li, A., Han, H., Liu, T., and Yang, Q. (2018) A potent chitinase from Bacillus subtilis for the efficient bioconversion of chitin-containing wastes. Int. J. Biol. Macromol. 116, 863–868
4. Cheng, C., Haider, J., Liu, P., Yang, J., Tan, Z., Huang, T., Lin, J., Jiang, M., Liu, H., and Zhu, L. (2020) Engineered LPMO Significantly Boosting Cellulase-Catalyzed Depolymerization of Cellulose. J. Agric. Food Chem. 10.1021/acs.jafc.0c05979
5. Chang, H. N., Kim, N. J., Kang, J., and Jeong, C. M. (2010) Biomass-derived volatile fatty acid platform for fuels and chemicals. Biotechnol. Bioprocess Eng. 15, 1–10

6. Kumar, M. N. V. R. (2000) A review of chitin and chitosan applications. Eng. Sci. Fundam. 2015 - Core Program. Area 2015 AIChE Annu. Meet. 46, 1–27
7. Kaczmarek, M. B., Struszczyk-Swita, K., Li, X., Szczęsna-Antczak, M., and Daroch, M. (2019) Enzymatic Modifications of Chitin, Chitosan, and Chitooligosaccharides. Front. Bioeng. Biotechnol. 10.3389/fbioe.2019.00243
8. Ben Amar Cheba (2011) Chitin and Chitosan: Marine Biopolymers with Unique Properties and Versatile Applications. Glob. J. Biotechnol. Biochem. 6, 149–153
9. Forsberg, Z., Nelson, C. E., Dalhus, B., Mekasha, S., Loose, J. S. M., Crouch, L. I., Røhr, Å. K., Gardner, J. G., Eijsink, V. G. H., and Vaaje-Kolstad, G. (2016) Structural and functional analysis of a lytic polysaccharide monooxygenase important for efficient utilization of chitin in Cellvibrio japonicus. J. Biol. Chem. 291, 7300–7312
10. Wong, E., Vaaje-Kolstad, G., Ghosh, A., Hurtado-Guerrero, R., Konarev, P. V., Ibrahim, A. F. M., Svergun, D. I., Eijsink, V. G. H., Chatterjee, N. S., and van Aalten, D. M. F. (2012) The Vibrio cholerae colonization factor GbpA possesses a modular structure that governs binding to different host surfaces. PLoS Pathog. 8, 1–12
11. Suginta, W., Chumjan, W., Mahendran, K. R., Janning, P., Schulte, A., and Winterhalter, M. (2013) Molecular Uptake of Chitooligosaccharides through Chitoporin from the Marine Bacterium Vibrio harveyi. PLoS One. 10.1371/journal.pone.0055126
12. Hemsworth, G. R., Ciano, L., Davies, G. J., and Walton, P. H. (2018) Production and spectroscopic characterization of lytic polysaccharide monooxygenases, 1st Ed., Elsevier Inc., 10.1016/bs.mie.2018.10.014
13. Vaaje-Kolstad, G., Horn, S. J., Van Aalten, D. M. F., Synstad, B., and Eijsink, V. G. H. (2005) The non-catalytic chitin-binding protein CBP21 from Serratia marcescens is essential for chitin degradation. J. Biol. Chem. 280, 28492–28497
14. Kuusk, S., Kont, R., Kuusk, P., Heering, A., Sørlie, M., Bissaro, B., Eijsink, V. G. H., and Väljamäe, P. (2019) Kinetic insights into the role of the reductant in H2O2-driven degradation of chitin by a bacterial lytic polysaccharide monooxygenase. J. Biol. Chem. 294, 1516–1528
15. Forsberg, Z., Sørlie, M., Petrović, D., Courtade, G., Aachmann, F. L., Vaaje-Kolstad, G., Bissaro, B., Røhr, Å. K., and Eijsink, V. G. (2019) Polysaccharide degradation by lytic polysaccharide monooxygenases. Curr. Opin. Struct. Biol. 59, 54–64
16. Jensen, M. S., Klinkenberg, G., Bissaro, B., Chylenski, P., Vaaje-Kolstad, G., Kvitvang, H. F., Nærdal, G. K., Sletta, H., Forsberg, Z., and Eijsink, V. G. H. (2019) Engineering chitinolytic activity into a cellulose-active lytic polysaccharide monooxygenase provides insights into substrate specificity. J. Biol. Chem. 294, 19349–19364
17. Lombard, V., Golaconda Ramulu, H., Drula, E., Coutinho, P. M., and Henrissat, B. (2014) The carbohydrate-active enzymes database (CAZy) in 2013. Nucleic Acids Res. 42, 490–495
18. Paradisi, A., Johnston, E. M., Tovborg, M., Nicoll, C. R., Ciano, L., Dowle, A., Mcmaster, J., Hancock, Y., Davies, G. J., and Walton, P. H. (2019) Formation of a Copper(II)-Tyrosyl Complex at the Active Site of Lytic Polysaccharide Monooxygenases following Oxidation by H2O2. J. Am. Chem. Soc. 141, 18585–18599
19. Zhang, H., Zhao, Y., Cao, H., Mou, G., and Yin, H. (2015) Expression and characterization of a lytic polysaccharide monooxygenase from Bacillus thuringiensis. Int. J. Biol. Macromol. 79, 72–75
20. Forsberg, Z., Mackenzie, A. K., Sørlie, M., Røhr, Å. K., Helland, R., Arvai, A. S., Vaaje-Kolstad, G., and Eijsink, V. G. H. (2014) Structural and functional characterization of a conserved pair of bacterial cellulose-oxidizing lytic polysaccharide monooxygenases. Proc. Natl. Acad. Sci. U. S. A. 111, 8446–8451
21. Watanabe, K. S. M. S. M. T. N. N. & T. (1998) Chitin binding protein (CBP21) in the culture supernatant of Serratia marcescens 2170. Biosci Biotechnol Biochem. 62, 128–135
22. Chaplin, A. K., Wilson, M. T., Hough, M. A., Svistunenko, D. A., Hemsworth, G. R., Walton, P. H., Vijgenboom, E., and Worrall, J. A. R. (2016) Heterogeneity in the Histidine-brace Copper Coordination Sphere in Auxiliary Activity Family 10 (AA10) Lytic Polysaccharide Monooxygenases. J. Biol. Chem. 10.1074/jbc.M116.722447
23. Singh, R. K., Blossom, B. M., Russo, D. A., Singh, R., Weihe, H., Andersen, N. H., Tiwari, M. K., Jensen, P. E., Felby, C., and Bjerrum, M. J. (2020) Detection and Characterization of a Novel Copper-Dependent Intermediate in a Lytic Polysaccharide Monooxygenase. Chem. - A Eur. J. 26, 454–463
24. Mutahir, Z., Mekasha, S., Loose, J. S. M., Abbas, F., Vaaje-Kolstad, G., Eijsink, V. G. H., and Forsberg, Z. (2018) Characterization and synergistic action of a tetra-modular lytic polysaccharide monooxygenase from Bacillus cereus. FEBS Lett. 592, 2562–2571
25. Crouch, L. I., Labourel, A., Walton, P. H., Davies, G. J., and Gilbert, H. J. (2016) The Contribution of Non-catalytic Carbohydrate Binding Modules to the Activity of Lytic Polysaccharide Monooxygenases. J. Biol. Chem. 10.1074/jbc.M115.702365
26. Meier, K. K., Jones, S. M., Kaper, T., Hansson, H., Koetsier, M. J., Karkehabadi, S., Solomon, E. I., Sandgren, M., and Kelemen, B. (2018) Oxygen Activation by Cu LPMOs in Recalcitrant Carbohydrate Polysaccharide Conversion to Monomer Sugars. Chem. Rev. 118, 2593–2635
27. Horn, S. J., Vaaje-kolstad, G., Westereng, B., and Eijsink, V. G. (2012) Novel enzymes for the degradation of cellulose. Biotechnol Biofuels. Biotechnol. Biofuels. 5, 45
28. Forsberg, Z. K. (2014) Discovery and characterization of cellulose-active lytic polysaccharide monooxygenases. Ph.D. thesis, Norwegian University of Life Sciences, 10.1038/nchembio.1417
29. Zhou, X., and Zhu, H. (2020) Current understanding of substrate specificity and regioselectivity of LPMOs. Bioresour. Bioprocess. 10.1186/s40643-020-0300-6
30. Meekrathok, P., Stubbs, K. A., Aunkham, A., Kaewmaneewat, A., Kardkuntod, A., Bulmer, D. M., van den Berg, B., and Suginta, W. (2020) NAG-thiazoline is a potent inhibitor of the Vibrio campbellii GH20 beta-N-Acetylglucosaminidase. FEBS J. 10.1111/febs.15283

31. Suginta, W., Robertson, P. A. W., Austin, B., Fry, S. C., and Fothergill-Gilmore, L. A. (2000) Chitinases from Vibrio: activity screening and purification of chiA from Vibrio carchariae. J. Appl. Microbiol. 10.1046/j.1365-2672.2000.01076.x
32. Li, X., and Roseman, S. (2004) The chitinolytic cascade in Vibrios is regulated by chitin oligosaccharides and a two-component chitin catabolic sensor/kinase. Proc. Natl. Acad. Sci. 10.1073/pnas.0307645100
33. Suginta, W., Khunkaewla, P., and Schulte, A. (2013) Electrochemical biosensor applications of polysaccharides chitin and chitosan. Chem. Rev. 113, 5458–5479
34. Kitaoku, Y., Nishimura, S., Hirono, T., Suginta, W., Ohnuma, T., and Fukamizo, T. (2019) Structures and chitin-binding properties of two N-terminal lysin motifs (LysMs) found in a chitinase from Volvox carteri. Glycobiology. 29, 565–575
35. Suginta, W., Chuenark, D., Mizuhara, M., and Fukamizo, T. (2010) Novel β-N-acetylglucosaminidases from Vibrio harveyi 650: Cloning, expression, enzymatic properties, and subsite identification. BMC Biochem. 10.1186/1471-2091-11-40
36. Suginta, W., Vongsuwan, A., Songsiriritthigul, C., Prinz, H., Estibeiro, P., Duncan, R. R., Svasti, J., and Fothergill-Gilmore, L. A. (2004) An endochitinase A from Vibrio carchariae: cloning, expression, mass and sequence analyses, and chitin hydrolysis. Arch. Biochem. Biophys. 10.1016/j.abb.2004.01.017
37. Suginta, W., Sirimontree, P., Sritho, N., Ohnuma, T., and Fukamizo, T. (2016) The chitin-binding domain of a GH-18 chitinase from Vibrio harveyi is crucial for chitin-chitinase interactions. Int. J. Biol. Macromol. 10.1016/j.ijbiomac.2016.09.066
38. LAEMMLI, U. K. (1970) Cleavage of Structural Proteins during the Assembly of the Head of Bacteriophage T4. Nature. 10.1038/227680a0
39. Paspaliari, D. K., Loose, J. S. M., Larsen, M. H., and Vaaje-Kolstad, G. (2015) Listeria monocytogenes has a functional chitinolytic system and an active lytic polysaccharide monooxygenase. FEBS J. 10.1111/febs.13191